Direct detection of WIMPs [*]

David G. Cerdeño[a], Anne M. Green[b]

[a] Departamento de Física Teórica C-XI, and Instituto de Física Teórica UAM-CSIC,
Universidad Autónoma de Madrid, Cantoblanco, E-28049 Madrid, Spain
[b] School of Physics and Astronomy, University of Nottingham
University Park, Nottingham, NG7 2RD, UK

February 9, 2010

Abstract

A generic weakly interacting massive particle (WIMP) is one of the most attractive candidates to account for the cold dark matter in our Universe, since it would be thermally produced with the correct abundance to account for the observed dark matter density. WIMPs can be searched for directly through their elastic scattering with a target material, and a variety of experiments are currently operating or planned with this aim. In these notes we overview the theoretical calculation of the direct detection rate of WIMPs as well as the different detection signals. We discuss the various ingredients (from particle physics and astrophysics) that enter the calculation and review the theoretical predictions for the direct detection of WIMPs in particle physics models.

1 Introduction

If the Milky Way's DM halo is composed of WIMPs, then the WIMP flux on the Earth is of order $10^5(100\,\mathrm{GeV}/m_\chi)\,\mathrm{cm}^{-2}\,\mathrm{s}^{-1}$. This flux is sufficiently large that, even though the WIMPs are weakly interacting, a small but potentially measurable fraction will elastically scatter off nuclei. Direct detection experiments aim to detect WIMPs via the nuclear recoils, caused by WIMP elastic scattering, in dedicated low background detectors [1]. More specifically they aim to measure the rate, R, and energies, E_R, of the nuclear recoils (and in directional experiments the directions as well).

In this chapter we overview the theoretical calculation of the direct detection event rate and the potential direct detection signals. Sec. 2 outlines the calculation of the event rate, including the spin independent and dependent contributions and the hadronic matrix elements. Sec. 3 discusses the astrophysical input into the event rate calculation, including the local WIMP velocity distribution and density. In Sec. 4 we describe the direction detection signals, specifically the energy, time and direction dependence of the event rate. Finally in Sec. 5 we discuss the predicted ranges for the WIMP mass and cross-sections in various particle physics models.

---

2 Event rate

The differential event rate, usually expressed in terms of counts/kg/day/keV (a quantity referred to as a differential rate unit or *dru*) for a WIMP with mass m_χ and a nucleus with mass m_N is given by

$$\frac{dR}{dE_R} = \frac{\rho_0}{m_N \, m_\chi} \int_{v_{min}}^{\infty} v f(v) \frac{d\sigma_{WN}}{dE_R}(v, E_R) \, dv \,, \qquad (1)$$

where ρ_0 is the local WIMP density, $\frac{d\sigma_{WN}}{dE_R}(v, E_R)$ is the differential cross-section for the WIMP-nucleus elastic scattering and $f(v)$ is the WIMP speed distribution in the detector frame normalized to unity.

Since the WIMP-nucleon relative speed is of order $100 \, \mathrm{km^{-1} \, s^{-1}}$ the elastic scattering occurs in the extreme non-relativistic limit, and the recoil energy of the nucleon is easily calculated in terms of the scattering angle in the center of mass frame, θ^*

$$E_R = \frac{\mu_N^2 v^2 (1 - \cos\theta^*)}{m_N} \,, \qquad (2)$$

where $\mu_N = m_\chi m_N / (m_\chi + m_N)$ is the WIMP-nucleus reduced mass.

The lower limit of the integration over WIMP speeds is given by the minimum WIMP speed which can cause a recoil of energy E_R: $v_{min} = \sqrt{(m_N E_R)/(2\mu_N^2)}$. The upper limit is formally infinite, however the local escape speed v_{esc} (see Sec. 3.2), is the maximum speed *in the Galactic rest frame* for WIMPs which are gravitationally bound to the Milky Way.

The total event rate (per kilogram per day) is found by integrating the differential event rate over all the possible recoil energies:

$$R = \int_{E_T}^{\infty} dE_R \frac{\rho_0}{m_N \, m_\chi} \int_{v_{min}}^{\infty} v f(v) \frac{d\sigma_{WN}}{dE_R}(v, E_R) \, dv \,, \qquad (3)$$

where E_T is the threshold energy, the smallest recoil energy which the detector is capable of measuring.

The WIMP-nucleus differential cross section encodes the particle physics inputs (and associated uncertainties) including the WIMP interaction properties. It depends fundamentally on the WIMP-quark interaction strength, which is calculated from the microscopic description of the model, in terms of an effective Lagrangian describing the interaction of the particular WIMP candidate with quarks and gluons. The resulting cross section is then promoted to a WIMP-nucleon cross section. This entails the use of hadronic matrix elements, which describe the nucleon content in quarks and gluons, and are subject to large uncertainties. In general, the WIMP-nucleus cross section can be separated into a spin-independent (scalar) and a spin-dependent contribution,

$$\frac{d\sigma_{WN}}{dE_R} = \left(\frac{d\sigma_{WN}}{dE_R}\right)_{SI} + \left(\frac{d\sigma_{WN}}{dE_R}\right)_{SD} \,. \qquad (4)$$

Finally, the total WIMP-nucleus cross section is calculated by adding coherently the above spin and scalar components, using nuclear wave functions. The form factor, $F(E_R)$, encodes the dependence on the momentum transfer, $q = \sqrt{2 m_N E_R}$, and accounts for the coherence

loss which leads to a suppression in the event rate for heavy WIMPs or nucleons. In general, we can express the differential cross section as

$$\frac{d\sigma_{WN}}{dE_R} = \frac{m_N}{2\mu_N^2 v^2} \left(\sigma_0^{SI} F_{SI}^2(E_R) + \sigma_0^{SD} F_{SD}^2(E_R) \right) , \qquad (5)$$

where $\sigma_0^{SI,SD}$ are the spin-independent and -dependent cross sections at zero momentum transfer.

The origin of the different contributions is best understood at the microscopic level, by analysing the Lagrangian which describes the WIMP interactions with quarks. The contributions to the spin-independent cross section arise from scalar and vector couplings to quarks, whereas the spin-dependent part of the cross section originates from axial-vector couplings. These contributions are characteristic of the particular WIMP candidate (see, e.g., [2]) and can be potentially useful for their discrimination in direct detection experiments.

2.1   Spin-dependent contribution

The contributions to the spin-dependent (SD) part of the WIMP-nucleus scattering cross section arise from couplings of the WIMP field to the quark axial current, $\bar{q}\gamma_\mu\gamma_5 q$. For example, if the WIMP is a (Dirac or Majorana) fermion, such as the lightest neutralino in supersymmetric models, the Lagrangian can contain the term

$$\mathcal{L} \supset \alpha_q^A (\bar{\chi}\gamma^\mu\gamma_5\chi)(\bar{q}\gamma_\mu\gamma_5 q). \qquad (6)$$

If the WIMP is a spin 1 field, such as in the case of LKP and LTP, the interaction term is slightly different,

$$\mathcal{L} \supset \alpha_q^A \epsilon^{\mu\nu\rho\sigma} (B_\rho \overset{\leftrightarrow}{\partial_\mu} B_\nu)(\bar{q}\gamma^\sigma\gamma_5 q). \qquad (7)$$

In both cases, the nucleus, N, matrix element reads

$$\langle N|\bar{q}\gamma_\mu\gamma_5 q|N\rangle = 2\lambda_q^N \langle N|J_N|N\rangle , \qquad (8)$$

where the coefficients λ_q^N relate the quark spin matrix elements to the angular momentum of the nucleons. They can be parametrized as

$$\lambda_q^N \simeq \frac{\Delta_q^{(p)}\langle S_p\rangle + \Delta_q^{(n)}\langle S_n\rangle}{J} , \qquad (9)$$

where J is the total angular momentum of the nucleus, the quantities Δq^n are related to the matrix element of the axial-vector current in a nucleon, $\langle n|\bar{q}\gamma_\mu\gamma_5 q|n\rangle = 2s_\mu^{(n)}\Delta_q^{(n)}$, and $\langle S_{p,n}\rangle = \langle N|S_{p,n}|N\rangle$ is the expectation value of the spin content of the proton or neutron group in the nucleus[1]. Adding the contributions from the different quarks, it is customary to define

$$a_p = \sum_{q=u,d,s} \frac{\alpha_q^A}{\sqrt{2}G_F}\Delta_q^p; \quad a_n = \sum_{q=u,d,s} \frac{\alpha_q^A}{\sqrt{2}G_F}\Delta_q^n , \qquad (10)$$

---

[1]These quantities can be determined from simple nuclear models. For example, the single-particle shell model assumes the nuclear spin is solely due to the spin of the single unpaired proton or neutron, and therefore vanishes for even nuclei. More accurate results can be obtained by using detailed nuclear calculations.

and

$$\Lambda = \frac{1}{J} \left[a_p \langle S_p \rangle + a_n \langle S_n \rangle \right] . \tag{11}$$

The resulting differential cross section can then be expressed (in the case of a fermionic WIMP) as

$$\left(\frac{d\sigma_{WN}}{dE_R} \right)_{SD} = \frac{16 m_N}{\pi v^2} \Lambda^2 G_F^2 J(J+1) \frac{S(E_R)}{S(0)} , \tag{12}$$

(using $d|\vec{q}|^2 = 2m_N dE_R$). The expression for a spin 1 WIMP can be found, e.g., in Ref. [2].

In the parametrization of the form factor it is common to use a decomposition into isoscalar, $a_0 = a_p + a_n$, and isovector, $a_1 = a_p - a_n$, couplings

$$S(q) = a_0^2 S_{00}(q) + a_0 a_1 S_{01}(q) + a_1^2 S_{11}(q) , \tag{13}$$

where the parameters S_{ij} are determined experimentally.

2.2   Spin-independent contribution

Spin-independent (SI) contributions to the total cross section may arise from scalar-scalar and vector-vector couplings in the Lagrangian:

$$\mathcal{L} \supset \alpha_q^S \bar{\chi} \chi \bar{q} q + \alpha_q^V \bar{\chi} \gamma_\mu \chi \bar{q} \gamma^\mu q . \tag{14}$$

The presence of these couplings depends on the particle physics model underlying the WIMP candidate. In general one can write

$$\left(\frac{d\sigma_{WN}}{dE_R} \right)_{SI} = \frac{m_N \sigma_0 F^2(E_R)}{2\mu_N^2 v^2} , \tag{15}$$

where the nuclear form factor for coherent interactions $F^2(E_R)$ can be qualitatively understood as a Fourier transform of the nucleon density and is usually parametrized in terms of the momentum transfer as [3; 4]

$$F^2(q) = \left(\frac{3 j_1(q R_1)}{q R_1} \right)^2 \exp \left[-q^2 s^2 \right] , \tag{16}$$

where j_1 is a spherical Bessel function, $s \simeq 1$ fm is a measure of the nuclear skin thickness, and $R_1 = \sqrt{R^2 - 5s^2}$ with $R \simeq 1.2\, A^{1/2}$ fm. The form factor is normalized to unity at zero momentum transfer, $F(0) = 1$.

The contribution from the scalar coupling leads to the following expression for the WIMP-nucleon cross section,

$$\sigma_0 = \frac{4\mu_N^2}{\pi} \left[Z f^p + (A - Z) f^n \right]^2 , \tag{17}$$

with

$$\frac{f^p}{m_p} = \sum_{q=u,d,s} \frac{\alpha_q^S}{m_q} f_{Tq}^p + \frac{2}{27} f_{TG}^p \sum_{q=c,b,t} \frac{\alpha_q^S}{m_q} , \tag{18}$$

where the quantities f_{Tq}^p represent the contributions of the light quarks to the mass of the proton, and are defined as $m_p f_{Tq}^p \equiv \langle p | m_q \bar{q} q | p \rangle$. Similarly the second term is due to the

interaction of the WIMP and the gluon scalar density in the nucleon, with $f_{TG}^p = 1 - \sum_{q=u,d,s} f_{Tq}^p$. They are determined experimentally,

$$f_{Tu}^p = 0.020 \pm 0.004, \quad f_{Td}^p = 0.026 \pm 0.005, \quad f_{Ts}^p = 0.118 \pm 0.062, \tag{19}$$

with $f_{Tu}^n = f_{Td}^p$, $f_{Td}^n = f_{Tu}^p$, and $f_{Ts}^n = f_{Ts}^p$. The uncertainties in these quantities, among which the most important is that on f_{Ts}, mainly stem from the determination of the π-nucleon sigma term.

The vector coupling (which is present, for example, in the case of a Dirac fermion but vanishes for Majorana particles) gives rise to an extra contribution. Interestingly, the sea quarks and gluons do not contribute to the vector current. Only valence quarks contribute, leading to the following expression

$$\sigma_0 = \frac{\mu_N^2 B_N^2}{64\pi}, \tag{20}$$

with

$$B_N \equiv \alpha_u^V (A + Z) + \alpha_d^V (2A - Z). \tag{21}$$

Thus, for a general WIMP with both scalar and vector interactions, the spin-independent contribution to the scattering cross section would read

$$\left(\frac{d\sigma_{WN}}{dE_R} \right)_{SI} = \frac{2\,m_N}{\pi v^2} \left[[Zf^p + (A - Z)f^n]^2 + \frac{B_N^2}{256} \right] F^2(E_R). \tag{22}$$

In most cases the WIMP coupling to neutrons and protons is very similar, $f^p \approx f^n$, and therefore the scalar contribution can be approximated by

$$\left(\frac{d\sigma_{WN}}{dE_R} \right)_{SI} = \frac{2\,m_N\,A^2(f^p)^2}{\pi v^2} F^2(E_R). \tag{23}$$

The spin-independent contribution basically scales as the square of the number of nucleons (A^2), whereas the spin-dependent one is proportional to a function of the nuclear angular momentum, $(J + 1)/J$. Although in general both have to be taken into account, the scalar component dominates for heavy targets ($A > 20$), which is the case for most experiments (usually based on targets with heavy nuclei such as Silicon, Germanium, Iodine or Xenon). Nevertheless, dedicated experiments exist that are also sensitive to the SD WIMP coupling through the choice of targets with a large nuclear angular momentum.

As we have seen, the WIMP direct detection rate depends on both astrophysical input (the local DM density and velocity distribution, in the lab frame) and particle physics input (nuclear form factors and interaction cross-sections, which depend on the theoretical framework in which the WIMP candidate arises). We will discuss these inputs in more detail in Secs. 3 and 5 respectively.

2.3   Hadronic Matrix Elements

The effect of uncertainties in the hadronic matrix elements has been studied in detail for the specific case of neutralino dark matter [5–9]. Concerning the SI cross section, the quantities f_{Tq}^p in Eq.(19) can be parametrized in terms of the π nucleon sigma term, $\Sigma_{\pi N}$, (see in this respect, e.g., Refs.[7; 9]) which, in terms of the u and d quark masses reads

$$\Sigma_{\pi N} = \frac{1}{2} (m_u + m_d) \langle N | \bar{u}u + \bar{d}d | N \rangle, \tag{24}$$

and is related to the strange quark scalar density in the nucleon. The largest source of uncertainty in f_{Tq}^p stems from the determination of this quantity, for which the current data implies $\Sigma_{\pi N} = (64 \pm 8)\,\text{MeV}$ [10], which translates into a variation of a factor 4 in f_{Ts}. Notice that in general the WIMP interaction with strange quarks would be the leading contribution to the SI cross section, due to its larger Yukawa coupling. In this case, σ_0 is roughly proportional to $f_{Ts}{}^2$ and the above uncertainty in the strange quark content leads to a variation of more than one order of magnitude in the resulting SI cross section [7; 9]).

Similarly, for the SD cross section the uncertainties in the strange spin contribution Δ_s are the dominant contribution to the error in σ_0. However, in the case of the neutralino, this can imply a correction of as much as a factor 2 in the resulting cross section [9], being therefore much smaller than the above uncertainty for the SI cross section. It should be emphasized, however, that uncertainties in the determination of the spin form factors $S(q)$ would also affect the theoretical predictions for the dark matter detection rate.

3 Astrophysics input

3.1 Local DM density

The differential event rate is directly proportional to the local WIMP density, $\rho_0 \equiv \rho(r = R_0)$ where $R_0 = (8.0 \pm 0.5)\,\text{kpc}$ [11] is the solar radius. Any observational uncertainty in ρ_0 therefore translates directly into in an uncertainty in the event rate and the inferred constraints on, or measurements of, the scattering cross-sections.

Exclusion limits are traditionally calculated assuming a canonical local WIMP density, $\rho_0 = 0.3\,\text{GeV}\,\text{cm}^{-3}$. The local WIMP density is calculated by applying observational constraints (including measurements of the rotation curve) to models of the Milky Way and the values obtained can vary by a factor or order 2 depending on the models used [12–15]. A recent study [16], using spherical halo models with a cusp ($\rho \propto r(r)^{-\alpha}$ as $r \to 0$) finds $\rho_0 = (0.30 \pm 0.05)\,\text{GeV}\,\text{cm}^{-3}$.

3.2 Speed distribution

The standard halo model, conventionally used in calculations of exclusion limits and signals, has an isotropic, Gaussian velocity distribution (often referred to as Maxwellian)

$$f(\mathbf{v}) = \frac{1}{\sqrt{2\pi}\sigma} \exp\left(-\frac{|\mathbf{v}|^2}{2\sigma^2}\right). \tag{25}$$

The speed dispersion is related to the local circular speed by $\sigma = \sqrt{3/2}v_c$ and $v_\text{c} = (220 \pm 20)\,\text{km}\,\text{s}^{-1}$ [17] (see Sec.3.3) so that $\sigma \approx 270\,\text{km}\,\text{s}^{-1}$. This velocity distribution corresponds to an isotropic singular isothermal sphere with density profile $\rho(r) \propto r^{-2}$. The isothermal sphere is simple, and not unreasonable as a first approximation, however it is unlikely to be an accurate model of the actual density and velocity distribution of the Milky Way. Observations and numerical simulations (see chapter 1) indicate that dark matter halos do not have a $1/r^2$ density profile and are (to some extent at least) triaxial and anisotropic.

If the velocity distribution is isotropic there is a one to one relation between $f(\mathbf{v})$ and the the spherically symmetric density profile given by Eddington's formula [18], see Refs. [19; 20]. In general the steady state phase-space distribution of a collection of collisionless particles

is given by the collisionless Boltzmann equation and the velocity dispersions of the system are calculated via the Jean's equations (e.g. Ref. [21]). Solving the Jean's equations requires assumptions to be made, and therefore even for a specific density distribution the solution is not unique. Several specific models have been used in the context of WIMP direct detection signals. The logarithmic ellipsoidal model [22] is the simplest triaxial generalisation of the isothermal sphere and has a velocity distribution which is a multi-variate Gaussian. Osipkov-Merritt models [23; 24] are spherically symmetric with radially dependent anisotropic velocity distributions. Fitting functions for the speed distributions in these models are available, for a selection of density profiles, in Ref. [25]. Velocity distributions have also been extracted from cosmological simulations, with both multi-variate Gaussian [26] and Tsallis [27] distributions [28] being advocated as fitting functions. While it is not known whether any of these models provide a good approximation to the real local velocity distribution function, the models are none the less useful for assessing the uncertainties in the direct detection signals.

Particles with speed, in the Galactic rest frame, greater than the local escape speed, $v_{esc} = \sqrt{2|\Phi(R_0)|}$ where $\Phi(r)$ is the potential, are not gravitationally bound. Many of the models used, in particular the standard halo model, formally extend to infinite radii and therefore their speed distribution has to be truncated at v_{esc} 'by hand' (see e.g. Ref. [29]). The standard value for the escape speed is $v_{esc} = 650 \, \text{km} \, \text{s}^{-1}$. A recent analysis, using high velocity stars from the RAVE survey, finds $498 \text{km} \, \text{s}^{-1} < v_{esc} < 608 \, \text{km} \, \text{s}^{-1}$ with a median likelihood of $544 \, \text{km} \, \text{s}^{-1}$ [30].

In Sec. 4 we discuss the impact of uncertainty in the speed distribution on the direct detection signals.

3.3 Earth's motion

The WIMP speed distribution in the detector rest frame is calculated by carrying out, a time dependent, Galilean transformation: $\mathbf{v} \to \tilde{\mathbf{v}} = \mathbf{v} + \mathbf{v}_e(t)$. The Earth's motion relative to the Galactic rest frame, $\mathbf{v}_e(t)$, is made up of three components: the motion of the Local Standard of Rest (LSR), the Sun's peculiar motion with respect to the LSR, $\mathbf{v}_\odot^{\text{p}}$, and the Earth's orbit about the Sun, $\mathbf{v}_e^{\text{orb}}$.

If the Milky Way is axisymmetric then the motion of the LSR is given by the local circular velocity $(0, v_c, 0)$, where $v_\text{c} = 220 \, \text{km} \, \text{s}^{-1}$ is the standard value. Kerr and Lynden-Bell found, by combining a large number of independent measurements, $v_\text{c} = (222 \pm 20) \, \text{km} \, \text{s}^{-1}$ [17]. A more recent determination, using the proper motions of Cepheids measured by Hipparcos [31], is broadly consistent: $v_c = (218 \pm 7) \, \text{km} \, \text{s}^{-1} (R_0/8 \, \text{kpc})$.

The Sun's peculiar motion, determined using the parallaxes and proper motions of stars in the solar neighbourhood from the Hipparcos catalogue, is $\mathbf{v}_\odot^{\text{p}} = (10.0 \pm 0.4, 5.2 \pm 0.6, 7.2 \pm 0.4) \, \text{km} \, \text{s}^{-1}$ [32] in Galactic co-ordinates (where x points towards the Galactic center, y is the direction of Galactic rotation and z towards the North Galactic Pole).

A relatively simple, and reasonably accurate, expression for the Earth's motion about the Sun can be found by ignoring the ellipticity of the Earth's orbit and the non-uniform motion of the Sun in right ascension [33]: $\mathbf{v}_e^{\text{orb}} = v_e[\mathbf{e}_1 \sin \lambda(t) - \mathbf{e}_2 \cos \lambda(t)]$ where $v_e = 29.8 \, \text{km} \, \text{s}^{-1}$ is the orbital speed of the Earth, $\lambda(t) = 2\pi(t - 0.218)$ is the Sun's ecliptic longitude (with t in years) and $\mathbf{e}_{1(2)}$ are unit vectors in the direction of the Sun at the Spring equinox (Summer solstice). In Galactic co-ordinates $\mathbf{e}_1 = (-0.0670, 0.4927, -0.8676)$ and $\mathbf{e}_2 = (-0.9931, -0.1170, 0.01032)$. More accurate expressions can be found in Ref. [34].

The main characteristics of the WIMP signals can be found using only the motion of the LSR, and for the time dependence the component of the Earth's orbital velocity in that direction. However accurate calculations, for instance for comparison with data, require all the components described above to be taken into account.

3.4 Ultra-fine structure

Most of the WIMP velocity distributions discussed in Sec. 3.2 are derived by solving the collisionless Boltzmann equation, which assumes that the phase space distribution has reached a steady state. However this may not be a good assumption for the Milky Way; structure formation in CDM cosmologies occurs hierarchically and the relevant dynamical timescales for the Milky Way are not many orders of magnitude smaller than the age of the Universe.

Both astronomical observations and numerical simulations (due to their finite resolution) typically probe the dark matter distribution on $\sim$ kpc scales. Direct detection experiments probe the DM distribution on sub milli-pc scales (the Earth's speed with respect to the Galactic rest frame is $\approx 0.2\,\mathrm{mpc\,yr^{-1}}$). It has been argued (see e.g. Refs. [35–37]) that on these scales the DM may not have yet reached a steady state and could have a non-smooth phase-space distribution. On the other hand it has been argued that the rapid decrease in density of streams evolving in a realistic, ellipsoidal, Galactic potential means that there will be a large number of overlapping streams in the solar neighbourhood producing an effectively smooth DM distribution [38].

If the local DM distribution consists of a small number of streams, rather than a smooth distribution, then there would be significant changes in the signals which we will discuss in Sec. 4. This is currently an open issue; directly calculating the DM distribution on the scales probed by direct detection experiments is a difficult and unresolved problem.

It has been suggested that a tidal stream from the Sagittarius (Sgr) dwarf galaxy, which is in the process of being disrupted, passes through the solar neighbourhood with the associated DM potentially producing distinctive signals in direct detection experiments [39; 40]. Subsequent numerical simulations of the disruption of Sgr along with observational searches for local streams of stars suggest that the Sgr stream does not in fact pass through the solar neighbourhood (see e.g. Ref. [41]). None the less the calculations of the resulting WIMP signals in Refs. [39; 40] provide a useful illustration of the qualitative effects of streams.

4 Signals

We have already seen in Sec. 2 that the recoil rate is energy dependent due to the kinematics of elastic scattering, combined with the WIMP speed distribution. Due to the motion of the Earth with respect to the Galactic rest frame the recoil rate is also both time and direction dependent. In this section we examine the energy, time and direction dependence of the recoil rate and the resulting WIMP signals. In each case we first focus on the signal expected for the standard halo model, with a Maxwellian velocity distribution, before discussing the effect on the signal of changes in the WIMP velocity distribution.

4.1 Energy dependence

The shape of the differential event rate depends on the WIMP and target masses, the WIMP velocity distribution and the form factor. For the standard halo model the expression for the differential event rate, eq. 1, can be rewritten approximately (c.f. Ref.[42]) as

$$\frac{\mathrm{d}R}{\mathrm{d}E_R} \approx \left(\frac{\mathrm{d}R}{\mathrm{d}E_R}\right)_0 F^2(E_R) \exp\left(-\frac{E_R}{E_c}\right), \qquad (26)$$

where $(\mathrm{d}R/\mathrm{d}E_R)_0$ is the event rate in the $E \to 0$ keV limit. The characteristic energy scale is given by $E_c = (c_1 2\mu_N^2 v_c^2)/m_N$ where c_1 is a parameter of order unity which depends on the target nuclei. If the WIMP is much lighter than the target nuclei, $m_\chi \ll m_N$, then $E_c \propto m_\chi^2/m_N$ while if the WIMP is much heavier than the target nuclei $E_c \propto m_N$. The total recoil rate is directly proportional to the WIMP number density, which varies as $1/m_\chi$.

In fig. 1 we plot the differential event rate for Ge and Xe targets and a range of WIMP masses. As expected, for a fixed target the differential event rate decreases more rapidly with increasing recoil energy for light WIMPs. For a fixed WIMP mass the decline of the differential event rate is steepest for heavy target nuclei. The dependence of the energy spectrum on the WIMP mass allows the WIMP mass to be estimated from the energies of detected events (e.g. Ref. [43]). Furthermore the consistency of energy spectra measured by experiments using different target nuclei would confirm that the events were due to WIMP scattering (rather than, for instance, neutron backgrounds) [42]. In particular, for spin independent interactions, the total event rate scales as A^2. The is sometimes referred to as the 'materials signal'.

The WIMP and target mass dependence of the differential event rate also have some general consequences for experiments. The dependence of the total event rate on m_χ means that, for fixed cross-section, a larger target mass will be required to detect heavy WIMPs than lighter WIMPs. For very light WIMPs the rapid decrease of the energy spectrum with increasing recoil energy means that the event rate above the detector threshold energy, E_T, may be small. If the WIMP is light, $< \mathcal{O}(10\,\text{GeV})$, a detector with a low, $< \mathcal{O}(\text{keV})$, threshold energy will be required.

The most significant astrophysical uncertainties in the differential event rate come from the uncertainties in the local WIMP density and circular velocity. As discussed in Sec. 3.1 the uncertainty in the local DM density translates directly into an uncertainty in constraints on (or in the future measurements of) the scattering cross-section. The *time averaged* differential event rate is found by integrating the WIMP velocity distribution, therefore it is only weakly sensitive to changes in the shape of the WIMP velocity distribution. For the smooth halo models discussed in Sec. 3.2 the *time averaged* differential event rates are fairly similar to that produced by the standard halo model [44; 45]. Consequently exclusion limits vary only weakly [45; 46] and there would be a small (of order a few per-cent) systematic uncertainty in the WIMP mass deduced from a measured energy spectrum [47]. With multiple detectors it would in principle be possible to measure the WIMP mass without any assumptions about the WIMP velocity distribution [48].

In the extreme case of the WIMP distribution being composed of a small number of streams the differential event rate would consists of a series of (sloping due to the form factor) steps. The positions of the steps would depend on the stream velocities and the target and WIMP masses, while the relative heights of the steps would depend on the stream densities.
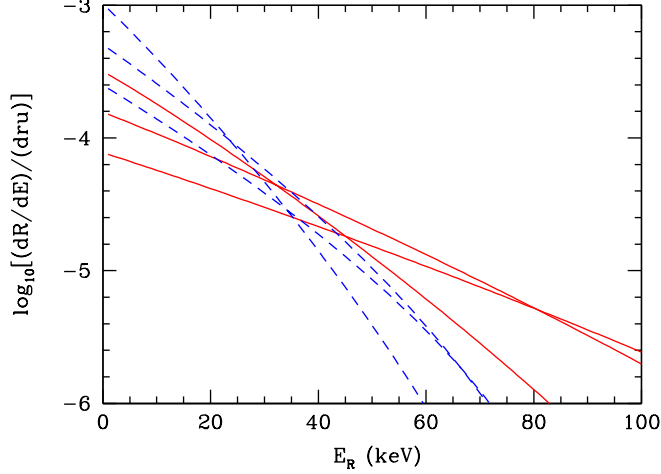
Figure 1: The dependence of the spin independent differential event rate on the WIMP mass and target. The solid and dashed lines are for Ge and Xe respectively and WIMP masses of (from top to bottom at $E_R = 0\,\text{keV}$) 50, 100 and 200 keV. The scattering cross-section on the proton is taken to be $\sigma_p^{SI} = 10^{-8}\,\text{pb}$.

4.2 Time dependence

The Earth's orbit about the Sun leads to a time dependence, specifically an annual modulation, in the differential event rate [29; 49]. The Earth's speed with respect to the Galactic rest frame is largest in Summer when the component of the Earth's orbital velocity in the direction of solar motion is largest. Therefore the number of WIMPs with high (low) speeds in the detector rest frame is largest (smallest) in Summer. Consequently the differential event rate has an annual modulation, with a peak in Winter for small recoil energies and in Summer for larger recoil energies [50]. The energy at which the annual modulation changes phase is often referred to as the 'crossing energy'.

Since the Earth's orbital speed is significantly smaller than the Sun's circular speed the amplitude of the modulation is small and, to a first approximation, the differential event rate can, for the standard halo model, be written approximately as a Taylor series:

$$\frac{\mathrm{d}R}{\mathrm{d}E_R} \approx \left(\frac{\mathrm{d}\bar{R}}{\mathrm{d}E_R} \right) \left[1 + \Delta(E_R) \cos \alpha(t) \right] , \qquad (27)$$

where $\alpha(t) = 2\pi(t - t_0)/T$, $T = 1$ year and $t_0 \sim 150$ days. In fig. 2 we plot the energy dependence of the amplitude in terms of $v_{\min}$ (recall that $v_{min} \propto E_R^{1/2}$ with the constant of proportionality depending on the WIMP and target nuclei masses). The amplitude of the modulation is of order 1-10 %.

The Earth's rotation provides another potential time dependence in the form of a diurnal modulation as the Earth acts as a shield in front of the detector [51; 52], however the
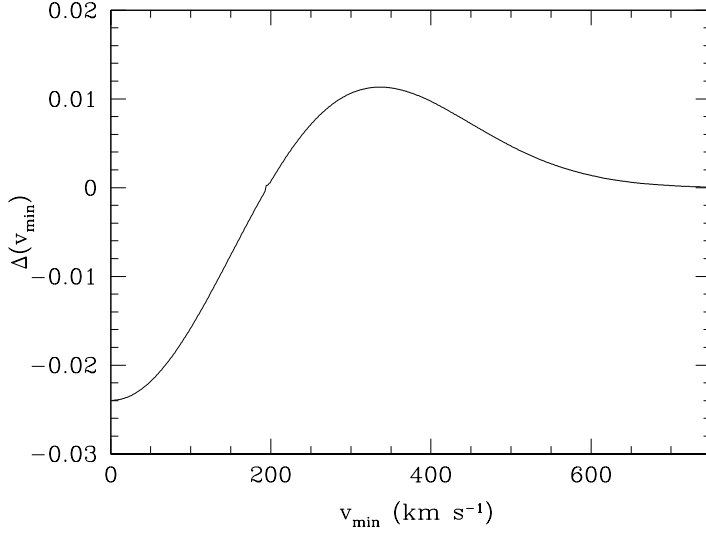
10

Figure 2: Dependence of the amplitude of the annual modulation, $\Delta(v_{\min})$, on $v_{\min}$.

amplitude of this effect is expected to be small, $< 1\%$ [52].

There has been a substantial amount of work on the annual modulation for the non-Maxwellian velocity distributions described in Sec. 3.2 [19; 20; 53–59]. In contrast to the time-averaged differential event rate, both the phase and amplitude of the annual modulation can vary substantially. Consequently the regions of WIMP mass-cross-section parameter space consistent with an observed signal can change significantly [54; 60]. Note that if the components of the Earth's orbital velocity perpendicular to the direction of Solar motion are neglected, then the phase change will be missed [57]. For a WIMP stream the position and height of the step in the energy spectrum would vary annually (e.g. Ref. [61]).

4.3 Direction dependence

The detector motion with respect to the Galactic rest frame also produces a directional signal. The WIMP flux in the lab frame is sharply peaked in the direction of motion of the Earth, and hence the recoil spectrum is also peaked in this direction (albeit less sharply due to the elastic scattering).

The directional recoil rate is most compactly written as [62]

$$\frac{\mathrm{d}R}{\mathrm{d}E_R \mathrm{d}\Omega} = \frac{\rho_0 \sigma_0 A^2}{4\pi\mu_p^2 m_\chi} F^2(E_R)\hat{f}(v_{\min}, \hat{\mathbf{q}}) \,, \tag{28}$$

where $\mathrm{d}\Omega = \mathrm{d}\phi\,\mathrm{d}\cos\theta$, $\hat{\mathbf{q}}$ is the recoil direction and $\hat{f}(v_{\min}, \hat{\mathbf{q}})$ is the 3-dimensional Radon transform of the WIMP velocity distribution $f(\mathbf{v})$

$$\hat{f}(v_{\min}, \hat{\mathbf{q}}) = \int \delta(\mathbf{v}.\hat{\mathbf{q}} - v_{\min}) f(\mathbf{v}) \mathrm{d}^3 v \,. \tag{29}$$

11

Geometrically the Radon transform is the integral of the function $f(\mathbf{v})$ on a plane orthogonal to the direction $\hat{\mathbf{q}}$ at a distance $v_{\min}$ from the origin. See Ref. [63] for an alternative, but equivalent, expression.

For the standard halo model the direction dependence is approximately given by [64]

$$\frac{\mathrm{d}R}{\mathrm{d}E_R \, \mathrm{d}\cos\gamma} \propto \exp\left[-\frac{(v_\odot \cos\gamma - v_{min})^2}{v_c^2}\right], \tag{30}$$

where γ is the angle between the recoil and the mean direction of solar motion. The distribution of recoil directions peaks in the mean direction of motion of the Sun (towards the constellation CYGNUS [65]) with the event rate in the forward direction being roughly an order of magnitude larger than that in the backward direction [64], since the Sun's speed is comparable to the mean WIMP speed. The directional recoil rate of $m_\chi = 100$ GeV WIMPs on S is shown in fig. 3.

With an ideal directional detector, with 3-d read-out and capable of measuring the senses of the recoils (*i.e.* distinguishing between the head and tail of each recoil), it would be possible to distinguish a WIMP signal from isotropic backgrounds with only of order 10 events [63; 66; 67]. This number increases significantly (by roughly an order of magnitude) if either the senses can not be measured or the read out is only 2-d [68–70]. Another potential directional signal is the rotation of the mean recoil direction in the lab over a sidereal day due to the motion of the Earth [65]. See chapter 22 for the principles and practice of directional detection experiments.

For plausible smooth halo models changes in the WIMP velocity distribution affect the detailed angular recoil rate. However the rear-front asymmetry is robust and the number of events required by an ideal detector only varies by of order 10% [63; 66; 67]. For non-ideal detectors the variation in the number of events required can be larger [67; 68]. With a large number of events (of order thousands) it would be possible to probe the detailed WIMP velocity distribution [67; 68; 71]. A stream of WIMPs produces a recoil spectrum which is peaked in the opposite direction (e.g. Ref. [72]).

5   Particle Physics input

Let us finally address the Particle Physics input to the determination of the WIMP detection rate, which enters through the theoretical predictions to the WIMP-nucleus scattering cross section. These are sensitive to the WIMP nature. We will here briefly summarise the results for WIMP candidates that arise in various well-motivated theories of physics beyond the Standard Model at the TeV scale (Supersymmetric theories, Universal Extra Dimension scenarios and Little Higgs models), as well as phenomenologically motivated scenarios.

5.1   Supersymmetric WIMPs

The canonical and best studied supersymmetric WIMP is the lightest neutralino, χ_1^0. Its detection properties are very dependent on its composition. More specifically, within the MSSM framework, in the expressions for the scattering amplitudes [6; 73–76], the SI part of the neutralino-nucleon cross section receives contributions from Higgs exchange in a t-channel and squark exchange in an s-channel. The latter also contributes to the SD part of the cross section, together with a Z boson exchange in a t-channel.
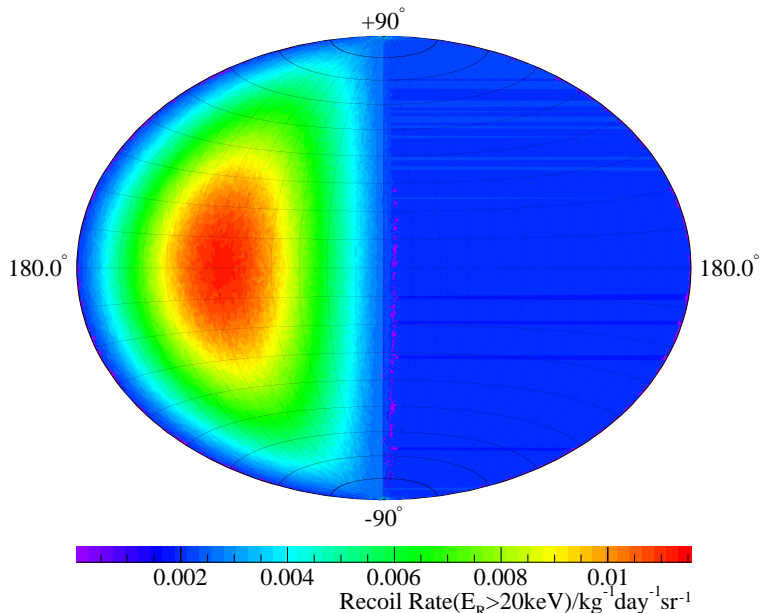
Figure 3: Hammer-Aitoff projection of the directional recoil rate for S, above $E_\mathrm{T} = 20\,\mathrm{keV}$, due to a standard halo of WIMPs with $m_\chi = 100\,\mathrm{GeV}$. This figure was generated using the HADES directional dark matter simulation code written by Ben Morgan.

The dependence of the cross sections, and detection prospects, on the neutralino composition are well known. For example, a large Higgsino component induces an enhancement of both the Higgs and Z boson exchange diagrams, thereby leading to an increase in both the SD and SI cross sections. On the other hand, the presence of light squarks (if they become almost degenerate with the neutralino) can lead to an enhancement of (mainly) the SD cross section.

Analyses of general supersymmetric scenarios with parameters defined at low energy reveal that the neutralino SI cross section can be as large as 10^{-5} pb for a wide range of neutralino masses up to 1 TeV [8; 77]. Interestingly, when gaugino masses not fulfilling the GUT relation are allowed, very light neutralinos with masses $m_{\chi_1^0} \gtrsim 7\,\mathrm{GeV}$, and potentially large cross-sections, can be obtained [78; 82]. It has been argued that these neutralinos could account for the DAMA/LIBRA annual modulation signal without contradicting the null results from CDMS and XENON10 [79], however this interpretation is now more constrained [80]. All these features are illustrated in in Fig.4.

Analyses have also been done from the point of view of Supergravity theories, where the SUSY parameters are defined at the GUT scale. In the simplest case, the CMSSM, the cross-sections are generally small, since χ_1^0 is mostly bino. The largest cross-sections, $\sigma^{SI} \approx \mathcal{O}(10^{-8}\,\mathrm{pb})$, are obtained in the focus point region, where the neutralino becomes a mixed bino-Higgsino state [83; 84]. Interestingly, this region seems to be favoured by recent Bayesian analyses of the CMSSM parameter space [85–88]. Moreover, the predicted SD cross section is also sizable in the focus point region, approximately reaching $10^{-4} - 10^{-3}$ pb. In more general Supergravity scenarios the predicted cross-sections can be significantly larger through the inclusion of non-universal values for either the scalar masses [89–104] (non-
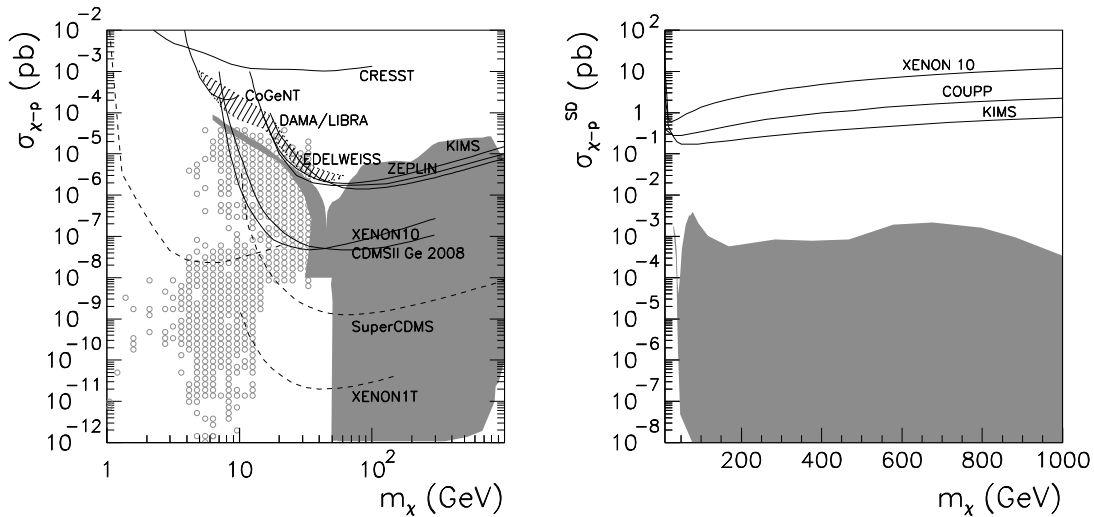
13

Figure 4: Left) Theoretical predictions for neutralino-nucleon SI cross section as a function of the neutralino mass obtained by combining the scans of the MSSM parameters from Refs.[8; 77–79]. The theoretical predictions for the SI cross section of very light neutralinos in the NMSSM from Ref. [80] are shown by means of empty grey circles. Present and projected experimental sensitivities are displayed using solid and dashed lines respectively. Right) Theoretical predictions for neutralino-nucleon SD cross section as a function of the neutralino mass, using the data from the supergravity scan of [81].

universalities in the Higgs mass parameters being the most effective), the gaugino masses [100; 105–109], or both [110; 111],

The detection prospects of the lightest neutralino in extended supersymmetric models may be significantly different, mostly due to the changes in the Higgs sector and the presence of new neutralino states. These constructions are generally referred to as singlet extensions of the MSSM (see, e.g., [112]) For example, this is the case of the NMSSM, in which the presence of very light Higgses (consistent with LEP constraints if they have a large singlet composition) can lead to a sizable increase of the SI cross section [113–115]. Moreover, in the NMSSM very light neutralinos (with masses below $10\,\text{GeV}$) are viable [116] and can have very distinctive predictions for their direct detection, including, for example, smaller SI cross section than in the MSSM [80]. The theoretical predictions for the SI cross section of neutralinos with $m_{\chi_1^0} \leq 30\,\text{GeV}$ are plotted in Fig.4. In general, the singlet component of the neutralino does not couple to the Z boson or to squarks and thus in these constructions the theoretical predictions for the SD cross section remain the same as in the MSSM.

Finally, there is another viable supersymmetric WIMP candidate for dark matter, the lightest sneutrino. The left-handed sneutrino in the MSSM is excluded given its sizable coupling to the Z boson. They therefore either annihilate too rapidly, resulting in a very small relic abundance, or have large scattering cross sections which have already been excluded by direct detection experiments [117]. Several models have been proposed to revive sneutrino DM by reducing its coupling with the Z-boson. This can be achieved by introducing a mixture of left- and right-handed sneutrinos [118–121], or by considering a purely right-handed sneutrino

14

in models with an extended gauge sector [122] or Higgs sector [123; 124] such as the NMSSM [125]. In the first class of models, the elastic scattering of sneutrinos with quarks would take place through the t-exchange of Z bosons, whereas in the second class it would mostly be due to the exchange of Higgs bosons. The resulting SI cross section in these cases can be within the reach of future detectors for a wide range of sneutrino masses [124; 125]. Being a scalar particle, the SD cross section vanishes for the sneutrino.

5.2 Kaluza Klein dark matter in UED

Models of Universal Extra Dimensions, in which all fields are allowed to propagate in the bulk [126], also provide well-motivated candidates for WIMP dark matter in the form of the Lightest Kaluza-Klein Particle (LKP), which is likely to be associated with the first KK excitation of the hypercharge gauge boson, $B_0^{(1)}$ [127; 128].

The elastic scattering of $B_0^{(1)}$ with quarks takes place through the exchange of KK quarks along t and s channels, which contribute to both the SD and SI cross section, and a Higgs exchange along a t-channel which only gives a SI contribution [129–131]. The theoretical predictions for the elastic scattering cross sections of $B_0^{(1)}$ are very dependent on the mass splitting between it and the KK quark, Δ_q. In particular, both the SI and SD contributions increase when Δ_q becomes small, as a consequence of the enhancement of the contribution from KK quarks. This is relevant, since in the UED scenario one expects a quasi-degenerate spectrum, in which the splittings between the masses are only induced by radiative corrections [127]. The SI cross section can also be larger in the presence of light Higgses and for small LKP masses. However the Higgs mass is generally larger than in the MSSM and its contribution is suppressed with respect to that of KK quarks.

It has been shown that the theoretical predictions for the SI cross section of $B_0^{(1)}$ can be as large as $\sigma^{SI} \approx 10^{-6}$ pb for masses ranging from 500 GeV to 1 TeV, when $\Delta_q \approx 0.01$, for which the correct relic density can be obtained [132; 133]. Under the same conditions, the predicted SD cross section are smaller and, for masses up to 1 TeV ton-scale detectors would be required to detect them. These predictions are illustrated in Fig. 5, from [134].

Other LKP candidates are possible within the UED model if nonvanishing boundary terms are allowed. More specifically, one may consider the first excited states associated with either the Z boson, $Z^{(1)}$, or the Higgs, $H^{(1)}$ [134]. The detection properties of the $Z^{(1)}$ are very similar to those of the $B_0^{(1)}$ [134] (although for the $Z^{(1)}$ the neutron and proton spin-dependent cross section are exactly the same, contrary to the case of the $B_0^{(1)}$).

Finally, in models with two universal extra dimensions the LKP generally corresponds to the KK excitation associated with the hypercharge gauge boson, which is called spinless photon [135]. Being a scalar, this particle has no SD cross section. Its SI cross section can be similar to that of the $B_0^{(1)}$.

5.3 Little Higgs dark matter

In these constructions a discrete symmetry, called T-parity, is introduced in order to alleviate the stringent experimental constraints on low-energy observables. A phenomenological consequence of T-parity is that the Lightest T-odd Particle (LTP) becomes absolutely stable. Interestingly, the LTP is usually the partner of the hypercharge gauge boson B_H [136–138].
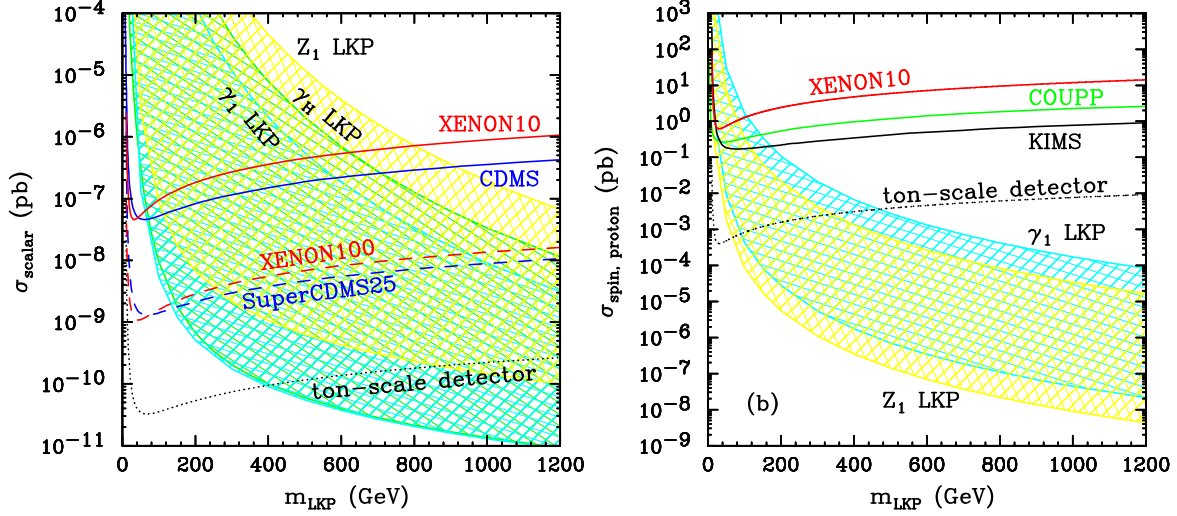
Figure 5: Left) Theoretical predictions for the SI LKP-nucleon scattering cross section as a function of the LKP mass for the LKP candidates discussed in the text. Right) Predictions for the SD LKP-proton cross section. Figures extracted from [134].

The LTP-nucleon scattering cross section receives SI contributions via Higgs and heavy quark exchange, the latter being the only contribution to the SD part [139]. Thus, the resulting expressions are very similar to the case of KK dark matter in UED. However, unlike the UED scenario, there is no reason for the heavy quarks to be degenerate in mass with A_H. This, together with the smallness of the heavy quark Yukawa couplings implies that their scattering cross-sections are in fact very suppressed. The SI cross section, being dominated by the Higgs exchange t-channel, increases slightly when the Higgs mass is small but is nevertheless generally below 10^{-10} pb. The theoretical predictions for the SD cross section are also very small. In summary, the direct detection of little Higgs dark matter is much more difficult than the SUSY and UED cases.

5.4 Minimal Models and other approaches for dark matter

Instead of considering DM candidates arising in existing theories beyond the SM, a bottom-up approach can be adopted in which minimal additions to the SM are considered, involving the inclusion of a WIMP field (usually a new singlet) and new symmetries that protect their decay (in some cases, also a new "mediator" sector that couples the WIMP to the SM). Examples in this direction include WIMPs with singlet mediation [140–142], models with an extended electroweak sector [143–145], models with additional gauge groups, and the Secluded Dark Matter scenario [146] in which WIMPs could escape direct detection.

The theoretical predictions for the direct detection of WIMPs in this class of models are very dependent on the mediator sector, since it determines the couplings of WIMPs to ordinary matter (quarks). For example, scalar WIMPs interact with ordinary quarks through the exchange of Higgs bosons in a t channel [140; 141]. The singlet coupling to the Higgs is constrained in order to reproduce the correct relic abundance, thus leaving only the WIMP and Higgs masses as free parameters. The resulting cross-sections increase as both masses decrease and can be as large as 10^{-6} pb for very light WIMPs of order 10 GeV but are reduced

16

to be below 10^{-8} pb when the DM candidate has a mass above $100\,\mathrm{GeV}$.

Other scenarios can have more general couplings. In the Inert Doublet Model, where elastic scattering proceeds only through the exchange of a Higgs or a Z boson along a t channel, the resulting SI cross section is rather small. Only for light WIMPs, with masses below $100\,\mathrm{GeV}$, is the predicted SI cross section large enough to be experimentally tested (from about 10^{-10} pb to as much as 10^{-7} pb) whereas the predictions for heavy WIMPs are well below the sensitivity of ton-size experiments, usually of order 10^{-13} pb [145].

In the Minimal DM approach of [143] WIMP candidates with direct couplings to the Z boson are already excluded by direct DM searches. However, some fermionic candidates are still viable which interact with quarks through the exchange of W (and Higgs) bosons. These particles (with masses of several TeV) can have an SI cross section of order 10^{-8} pb.

5.5 Inelastic cross section

It is finally worth mentioning that the WIMP-nucleon cross section can also receive a contribution from inelastic scattering by creating either an excited nuclear [147] or electronic state [148] or even by creating an excited WIMP state [149–151]. The last possibility is particularly interesting if the mass difference, δ, between the excited dark matter candidate, χ_2 and WIMP χ_1 is of order of the WIMP kinetic energy (i.e., about $100\,\mathrm{keV}$). In that case, the inelastic scattering off nuclei $\chi_1 N \to \chi_2 N$ can occur and the only kinematic change is in the minimal WIMP velocity that can trigger a specific recoil energy, which is increased by $\Delta v_{min} = \delta/\sqrt{(2m_N E_R)}$. This clearly favours detection in heavy targets such as Iodine (since Δv_{min} is smaller) and might provide a possible explanation for the DAMA/LIBRA signal compatible with the null restuls in other experiments [151].

5.6 Discrimination of Dark Matter candidates

As illustrated by figs. 4 and 5, current experiments are already probing the masses and cross-sections predicted for various WIMP candidates. Furthermore future experiments will be sensitive to a substantial fraction of the parameter space. If any of these experiments succeed in detecting dark matter particles, the next objective will be to identify its particle nature.

In this sense, the simultaneous measurement of both the SI and SD dark matter couplings, through experiments which are sensitive to both signals, can provide very valuable information [81]. This is illustrated in Fig. 6, where the ratio of SI to SD cross section is plotted for the neutralino and LKP cases versus the event rate for two complementary choices of target materials (that could be used in the COUPP experiment). As shown in the left panel, the measurement of an event rate in a single detector does reduce the number of allowed models, but does not generally place significant constraints on coupling parameters or on the nature of the dark matter detected. However, as shown in the right panel, a subsequent detection using a second complementary target does substantially reduce the allowed range of coupling parameters, and allows, in most cases, an effective discrimination between neutralino and LKP candidates.

This analysis can be extended to other dark matter candidates. Moreover, in order to eliminate the large astrophysical and theoretical uncertainties which affect the dark matter rates, the ratio of WIMP-proton and WIMP-neutron amplitudes can be used [152] and compared for different target materials. For example, the comparative study of the ratios of SD
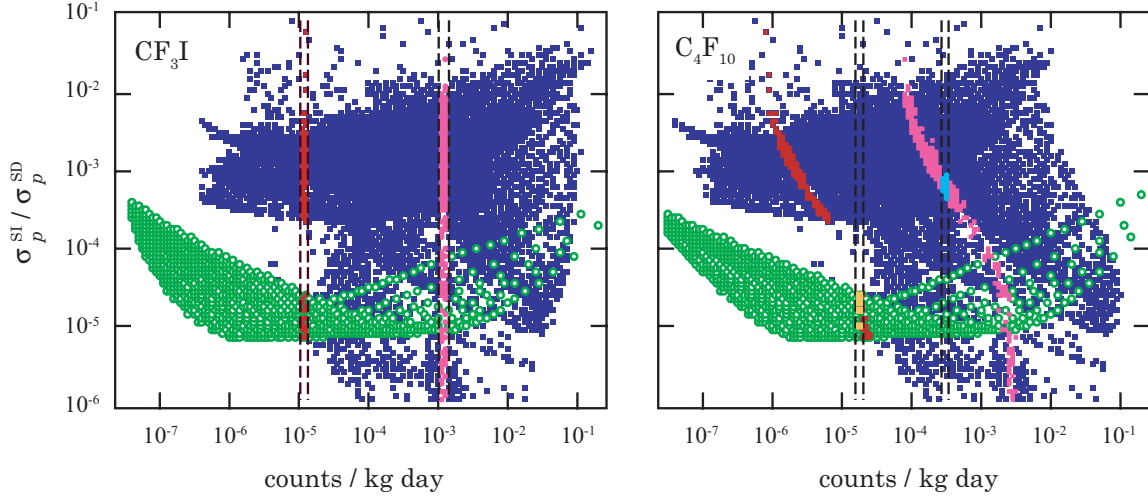
17

Figure 6: Left) The detection with a given target such as CF_3I can only loosely constrain models for the dark matter (blue squares for neutralinos, green circles for the LKP) in the $\sigma_p^{SI}/\sigma_p^{SD}$ versus count-rate plane. Red (magenta) dots show the many models consistent with a measurement of $\sim 10^{-5}$ (10^{-3}) counts/kg day. Right) measurement of the event rate in a second target such as C_4F_{10}, with lower sensitivity to spin-independent couplings, effectively reduces the remaining number of allowed models–orange (aqua) dots–and generally allows discrimination between the neutralino and the LKP. Figures extracted from [81].

neutron to proton amplitudes can provide a good discrimination of dark matter models by distinguishing candidates for which the SD cross section is dominated by Z boson exchange (such as the neutralino in some regions of the parameter space) from those where the dominant channel is squark or KK quark exchange (such as the LKP or LTP). A similar analysis for the SI neutron to proton ratio can be used to disentangle models with dominant Higgs or Z boson exchange, however in practise the different target materials are less sensitive to these differences. Finally, the mass determination techniques described in the Sec. 4.1 can provide complementary information that could lead to more effective discrimination between the various dark matter models.

References

[1] M. W. Goodman and E. Witten, "Detectability of certain dark-matter candidates," *Phys. Rev.*, vol. D31, p. 3059, 1985.

[2] V. Barger, W.-Y. Keung, and G. Shaughnessy, "Spin Dependence of Dark Matter Scattering," *Phys. Rev.*, vol. D78, p. 056007, 2008.

[3] R. H. Helm, "Inelastic and Elastic Scattering of 187-Mev Electrons from Selected Even-Even Nuclei," *Phys. Rev.*, vol. 104, pp. 1466–1475, 1956.

[4] J. Engel, "Nuclear form-factors for the scattering of weakly interacting massive particles," *Phys. Lett.*, vol. B264, pp. 114–119, 1991.

[5] A. Bottino, F. Donato, N. Fornengo, and S. Scopel, "Implications for relic neutralinos of the theoretical uncertainties in the neutralino nucleon cross-section," *Astropart. Phys.*, vol. 13, pp. 215–225, 2000.

[6] J. R. Ellis, A. Ferstl, and K. A. Olive, "Re-evaluation of the elastic scattering of supersymmetric dark matter," *Phys. Lett.*, vol. B481, pp. 304–314, 2000.

[7] A. Bottino, F. Donato, N. Fornengo, and S. Scopel, "Size of the neutralino nucleon cross-section in the light of a new determination of the pion nucleon sigma term," *Astropart. Phys.*, vol. 18, pp. 205–211, 2002.

[8] J. R. Ellis, K. A. Olive, Y. Santoso, and V. C. Spanos, "Update on the direct detection of supersymmetric dark matter," *Phys. Rev.*, vol. D71, p. 095007, 2005.

[9] J. R. Ellis, K. A. Olive, and C. Savage, "Hadronic Uncertainties in the Elastic Scattering of Supersymmetric Dark Matter," *Phys. Rev.*, vol. D77, p. 065026, 2008.

[10] M. M. Pavan, I. I. Strakovsky, R. L. Workman, and R. A. Arndt, "The pion nucleon Sigma term is definitely large: Results from a GWU analysis of pi N scattering data," *PiN Newslett.*, vol. 16, pp. 110–115, 2002.

[11] M. J. Reid, "The distance to the center of the galaxy," *Ann. Rev. Astron. Astrophys.*, vol. 31, pp. 345–372, 1993.

[12] J. A. R. Caldwell and J. P. Ostriker, "The Mass distribution within our Galaxy: A Three component model," *Astrophys. J.*, vol. 251, pp. 61–87, 1981.

[13] J. N. Bahcall, M. Schmidt, and R. M. Soneira, "The Galactic Spheroid," *Ap. J.*, vol. 265, p. 730, 1983.

[14] E. I. Gates, G. Gyuk, and M. S. Turner, "The Local halo density," *Astrophys. J.*, vol. 449, pp. L123–L126, 1995.

[15] L. Bergstrom, P. Ullio, and J. H. Buckley, "Observability of gamma rays from dark matter neutralino annihilations in the Milky Way halo," *Astropart. Phys.*, vol. 9, pp. 137–162, 1998.

[16] L. M. Widrow, B. Pym, and J. Dubinski, "Dynamical Blueprints for Galaxies," *Astrophys. J.*, vol. 679, pp. 1239–1259, 2008.

[17] F. J. Kerr and D. Lynden-Bell, "Review of galactic constants," *Mon. Not. Roy. Astron. Soc.*, vol. 221, p. 1023, 1986.

[18] A. S. Eddinton, "The distribution of stars in globular clusters," *Mon. Not. Roy. Astron. Soc.*, vol. 76, p. 572, 1916.

[19] P. Ullio and M. Kamionkowski, "Velocity distributions and annual-modulation signatures of weakly interacting massive particles," *JHEP*, vol. 03, p. 049, 2001.

[20] J. D. Vergados and D. Owen, "New velocity distribution for cold dark matter in the context of the Eddington theory," *Astrophys. J.*, vol. 589, pp. 17–28, 2003.

[21] J. Binney and S. Tremaine, "Galactic Dynamics," 2008.

[22] N. W. Evans, C. M. Carollo, and P. T. de Zeeuw, "Triaxial haloes and particle dark matter detection," *Mon. Not. Roy. Astron. Soc.*, vol. 318, p. 1131, 2000.

[23] L. P. Osipkov, "Spherical stellar systems with spheroidal velocity distributions," *Pis'ma Astron.*, vol. 55, p. 77, 1979.

[24] D. Merritt, "Spherical stellar systems with spheroidal velocity distributions," *Mon. Not. Roy. Astron. Soc.*, vol. 90, p. 1027, 1984.

[25] L. M. Widrow, "Distribution Functions for Cuspy Dark Matter Density Profiles," *Astrophys. J. Suppl. Series.*, p. 39, 2000.

[26] A. Helmi, S. D. M. White, and V. Springel, "The phase-space structure of a dark-matter halo: Implications for dark-matter direct detection experiments," *Phys. Rev.*, vol. D66, p. 063502, 2002.

[27] C. Tsallis, "Possible Generalization of Boltzmann-Gibbs Statistics," *J. Stat. Phys.*, vol. 52, pp. 479–487, 1988.

[28] S. H. Hansen, B. Moore, M. Zemp, and J. Stadel, "A universal velocity distribution of relaxed collisionless structures," *JCAP*, vol. 0601, p. 014, 2006.

[29] A. K. Drukier, K. Freese, and D. N. Spergel, "Detecting Cold Dark Matter Candidates," *Phys. Rev.*, vol. D33, pp. 3495–3508, 1986.

[30] M. C. Smith *et al.*, "The RAVE Survey: Constraining the Local Galactic Escape Speed," *Mon. Not. Roy. Astron. Soc.*, vol. 379, pp. 755–772, 2007.

[31] M. Feast and W. P., "Galactic kinematics of Cepheids from HIPPARCOS proper motions," *Mon. Not. Roy. Astron. Soc.*, vol. 291, p. 683, 1997.

[32] W. Dehnen and J. Binney, "Local stellar kinematics from Hipparcos data," *Mon. Not. Roy. Astron. Soc.*, vol. 298, pp. 387–394, 1998.

[33] G. Gelmini and P. Gondolo, "WIMP annual modulation with opposite phase in late-infall halo models," *Phys. Rev.*, vol. D64, p. 023504, 2001.

[34] R. M. Green, "Spherical astronomy," 1985.

[35] B. Moore *et al.*, "Dark matter in Draco and the Local Group: Implications for direct detection experiments," *Phys. Rev.*, vol. D64, p. 063508, 2001.

[36] D. Stiff and L. M. Widrow, "Fine Structure of Dark Matter Halos and its Effect on Terrestrial Detection Experiments," *Phys. Rev. Lett.*, vol. 90, p. 211301, 2003.

[37] D. S. M. Fantin, M. R. Merrifield, and A. M. Green, "Modelling ultra-fine structure in dark matter halos," *Mon. Not. Roy. Astron. Soc.*, vol. 390, p. 1055, 2008.

[38] M. Vogelsberger, S. D. M. White, A. Helmi, and V. Springel, "The fine-grained phase-space structure of Cold Dark Matter halos," *Mon. Not. Roy. Astron. Soc.*, vol. 385, pp. 236–254, 2008.

[39] K. Freese, P. Gondolo, and H. J. Newberg, "Detectability of weakly interacting massive particles in the Sagittarius dwarf tidal stream," *Phys. Rev.*, vol. D71, p. 043516, 2005.

[40] K. Freese, P. Gondolo, H. J. Newberg, and M. Lewis, "The Effects of the Sagittarius Dwarf Tidal Stream on Dark Matter Detectors," *Phys. Rev. Lett.*, vol. 92, p. 111301, 2004.

[41] G. M. Seabroke *et al.*, "Is the sky falling? Searching for stellar streams in the local Milky Way disc in the CORAVEL and RAVE surveys," *Mon. Not. Roy. Astron. Soc.*, vol. 382, pp. 11–32, 2007.

[42] J. D. Lewin and P. F. Smith, "Review of mathematics, numerical factors, and corrections for dark matter experiments based on elastic nuclear recoil," *Astropart. Phys.*, vol. 6, pp. 87–112, 1996.

[43] A. M. Green, "Determining the WIMP mass using direct detection experiments," *JCAP*, vol. 0708, p. 022, 2007.

[44] M. Kamionkowski and A. Kinkhabwala, "Galactic halo models and particle dark matter detection," *Phys. Rev.*, vol. D57, pp. 3256–3263, 1998.

[45] F. Donato, N. Fornengo, and S. Scopel, "Effects of galactic dark halo rotation on WIMP direct detection," *Astropart. Phys.*, vol. 9, pp. 247–260, 1998.

[46] A. M. Green, "Effect of halo modelling on WIMP exclusion limits," *Phys. Rev.*, vol. D66, p. 083003, 2002.

[47] A. M. Green, "Determining the WIMP mass from a single direct detection experiment, a more detailed study," *JCAP*, vol. 0807, p. 005, 2008.

[48] M. Drees and C.-L. Shan, "Model-Independent Determination of the WIMP Mass from Direct Dark Matter Detection Data," *JCAP*, vol. 0806, p. 012, 2008.

[49] K. Freese, J. A. Frieman, and A. Gould, "Signal Modulation in Cold Dark Matter Detection," *Phys. Rev.*, vol. D37, p. 3388, 1988.

[50] J. R. Primack, D. Seckel, and B. Sadoulet, "Detection of Cosmic Dark Matter," *Ann. Rev. Nucl. Part. Sci.*, vol. 38, pp. 751–807, 1988.

[51] J. I. Collar and F. T. Avignone, "Diurnal modulation effects in cold dark matter experiments," *Phys. Lett.*, vol. B275, pp. 181–185, 1992.

[52] F. Hasenbalg *et al.*, "Cold dark matter identification: Diurnal modulation revisited," *Phys. Rev.*, vol. D55, pp. 7350–7355, 1997.

[53] M. Brhlik and L. Roszkowski, "WIMP velocity impact on direct dark matter searches," *Phys. Lett.*, vol. B464, pp. 303–310, 1999.

[54] P. Belli *et al.*, "Extending the DAMA annual-modulation region by inclusion of the uncertainties in astrophysical velocities," *Phys. Rev.*, vol. D61, p. 023512, 2000.

[55] J. D. Vergados, "Modulation effect with realistic velocity dispersion of supersymmetric dark matter," *Phys. Rev. Lett.*, vol. 83, pp. 3597–3600, 1999.

[56] A. M. Green, "The WIMP annual modulation signal and non-standard halo models," *Phys. Rev.*, vol. D63, p. 043005, 2001.

[57] A. M. Green, "Effect of realistic astrophysical inputs on the phase and shape of the WIMP annual modulation signal," *Phys. Rev.*, vol. D68, p. 023004, 2003.

[58] J. D. Vergados, S. H. Hansen, and O. Host, "The impact of going beyond the Maxwell distribution in direct dark matter detection rates," *Phys. Rev.*, vol. D77, p. 023509, 2008.

[59] M. Fairbairn and T. Schwetz, "Spin-independent elastic WIMP scattering and the DAMA annual modulation signal," *JCAP*, vol. 0901, p. 037, 2009.

[60] P. Belli, R. Cerulli, N. Fornengo, and S. Scopel, "Effect of the galactic halo modeling on the DAMA/NaI annual modulation result: An extended analysis of the data for WIMPs with a purely spin-independent coupling," *Phys. Rev.*, vol. D66, p. 043503, 2002.

[61] C. Savage, K. Freese, and P. Gondolo, "Annual Modulation of Dark Matter in the Presence of Streams," *Phys. Rev.*, vol. D74, p. 043531, 2006.

[62] P. Gondolo, "Recoil momentum spectrum in directional dark matter detectors," *Phys. Rev.*, vol. D66, p. 103513, 2002.

[63] C. J. Copi and L. M. Krauss, "Angular signatures for galactic halo WIMP scattering in direct detectors: Prospects and challenges," *Phys. Rev.*, vol. D63, p. 043507, 2001.

[64] D. N. Spergel, "The motion of the Earth and the detection of WIMPs," *Phys. Rev.*, vol. D37, p. 1353, 1988.

[65] D. P. Snowden-Ifft, C. J. Martoff, and J. M. Burwell, "Low pressure negative ion drift chamber for dark matter search," *Phys. Rev.*, vol. D61, p. 101301, 2000.

[66] C. J. Copi, J. Heo, and L. M. Krauss, "Directional sensitivity, WIMP detection, and the galactic halo," *Phys. Lett.*, vol. B461, pp. 43–48, 1999.

[67] B. Morgan, A. M. Green, and N. J. C. Spooner, "Directional statistics for WIMP direct detection," *Phys. Rev.*, vol. D71, p. 103507, 2005.

[68] B. Morgan and A. M. Green, "Directional statistics for WIMP direct detection. II: 2-d read-out," *Phys. Rev.*, vol. D72, p. 123501, 2005.

[69] A. M. Green and B. Morgan, "Optimizing WIMP directional detectors," *Astropart. Phys.*, vol. 27, pp. 142–149, 2007.

[70] C. J. Copi, L. M. Krauss, D. Simmons-Duffin, and S. R. Stroiney, "Assessing Alternatives for Directional Detection of a WIMP Halo," *Phys. Rev.*, vol. D75, p. 023514, 2007.

[71] O. Host and S. H. Hansen, "What it takes to measure a fundamental difference between dark matter and baryons: the halo velocity anisotropy," *JCAP*, vol. 0706, p. 016, 2007.

[72] M. S. Alenazi and P. Gondolo, "Directional recoil rates for WIMP direct detection," *Phys. Rev.*, vol. D77, p. 043532, 2008.

[73] M. Srednicki and R. Watkins, "Coherent couplings of neutralinos to nuclei from squark mixing," *Phys. Lett.*, vol. B225, p. 140, 1989.

[74] G. B. Gelmini, P. Gondolo, and E. Roulet, "Neutralino dark matter searches," *Nucl. Phys.*, vol. B351, pp. 623–644, 1991.

[75] M. Drees and M. M. Nojiri, "New contributions to coherent neutralino - nucleus scattering," *Phys. Rev.*, vol. D47, pp. 4226–4232, 1993.

[76] M. Drees and M. Nojiri, "Neutralino-Nucleon Scattering Revisited," *Phys. Rev.*, vol. D48, pp. 3483–3501, 1993.

[77] Y. G. Kim, T. Nihei, L. Roszkowski, and R. Ruiz de Austri, "Upper and lower limits on neutralino WIMP mass and spin- independent scattering cross section, and impact of new (g- 2)(mu) measurement," *JHEP*, vol. 12, p. 034, 2002.

[78] A. Bottino, F. Donato, N. Fornengo, and S. Scopel, "Light neutralinos and WIMP direct searches," *Phys. Rev.*, vol. D69, p. 037302, 2004.

[79] A. Bottino, F. Donato, N. Fornengo, and S. Scopel, "Interpreting the recent results on direct search for dark matter particles in terms of relic neutralino," *Phys. Rev.*, vol. D78, p. 083520, 2008.

[80] C. E. Aalseth *et al.*, "Experimental constraints on a dark matter origin for the DAMA annual modulation effect," *Phys. Rev. Lett.*, vol. 101, p. 251301, 2008.

[81] G. Bertone, D. G. Cerdeño, J. I. Collar, and B. C. Odom, "WIMP identification through a combined measurement of axial and scalar couplings," *Phys. Rev. Lett.*, vol. 99, p. 151301, 2007.

[82] A. Bottino, N. Fornengo, and S. Scopel, "Light relic neutralinos," *Phys. Rev.*, vol. D67, p. 063519, 2003.

[83] J. Edsjo, M. Schelke, and P. Ullio, "Direct versus indirect detection in mSUGRA with self- consistent halo models," *JCAP*, vol. 0409, p. 004, 2004.

[84] H. Baer, T. Krupovnickas, S. Profumo, and P. Ullio, "Model independent approach to focus point supersymmetry: From dark matter to collider searches," *JHEP*, vol. 10, p. 020, 2005.

[85] R. R. de Austri, R. Trotta, and L. Roszkowski, "A Markov chain Monte Carlo analysis of the CMSSM," *JHEP*, vol. 05, p. 002, 2006.

[86] L. Roszkowski, R. Ruiz de Austri, and R. Trotta, "Implications for the Constrained MSSM from a new prediction for b to s gamma," *JHEP*, vol. 07, p. 075, 2007.

[87] B. C. Allanach and D. Hooper, "Panglossian Prospects for Detecting Neutralino Dark Matter in Light of Natural Priors," *JHEP*, vol. 10, p. 071, 2008.

[88] R. Trotta, F. Feroz, M. P. Hobson, L. Roszkowski, and R. Ruiz de Austri, "The impact of priors and observables on parameter inferences in the Constrained MSSM," *JHEP*, vol. 12, p. 024, 2008.

[89] V. Berezinsky *et al.*, "Neutralino dark matter in supersymmetric models with non–universal scalar mass terms," *Astropart. Phys.*, vol. 5, pp. 1–26, 1996.

[90] M. Drees, M. M. Nojiri, D. P. Roy, and Y. Yamada, "Light Higgsino dark matter," *Phys. Rev.*, vol. D56, pp. 276–290, 1997.

[91] P. Nath and R. L. Arnowitt, "Non-universal soft SUSY breaking and dark matter," *Phys. Rev.*, vol. D56, pp. 2820–2832, 1997.

[92] A. Bottino, F. Donato, N. Fornengo, and S. Scopel, "Compatibility of the new DAMA/NaI data on an annual modulation effect in WIMP direct search with a relic neutralino in supergravity schemes," *Phys. Rev.*, vol. D59, p. 095004, 1999.

[93] R. L. Arnowitt and P. Nath, "Annual modulation signature for the direct detection of Milky Way wimps and supergravity models," *Phys. Rev.*, vol. D60, p. 044002, 1999.

[94] E. Accomando, R. L. Arnowitt, B. Dutta, and Y. Santoso, "Neutralino proton cross sections in supergravity models," *Nucl. Phys.*, vol. B585, pp. 124–142, 2000.

[95] J. R. Ellis, K. A. Olive, and Y. Santoso, "The MSSM Parameter Space with Non-Universal Higgs Masses," *Phys. Lett.*, vol. B539, pp. 107–118, 2002.

[96] J. R. Ellis, T. Falk, K. A. Olive, and Y. Santoso, "Exploration of the MSSM with Non-Universal Higgs Masses," *Nucl. Phys.*, vol. B652, pp. 259–347, 2003.

[97] M. Drees, Y. G. Kim, T. Kobayashi, and M. M. Nojiri, "Direct detection of neutralino dark matter and the anomalous dipole moment of the muon," *Phys. Rev.*, vol. D63, p. 115009, 2001.

[98] J. R. Ellis, A. Ferstl, K. A. Olive, and Y. Santoso, "Direct Detection of Dark Matter in the MSSM with Non- Universal Higgs Masses," *Phys. Rev.*, vol. D67, p. 123502, 2003.

[99] R. L. Arnowitt and B. Dutta, "Dark matter detection rates in SUGRA models," 2001.

[100] D. G. Cerdeño, E. Gabrielli, and C. Muñoz, "Experimental constraints on the neutralino nucleon cross section," 2002.

[101] R. Dermisek, S. Raby, L. Roszkowski, and R. Ruiz De Austri, "Dark matter and $B/s \to \mu^+\mu^-$ with minimal SO(10) soft SUSY breaking," *JHEP*, vol. 04, p. 037, 2003.

[102] H. Baer, C. Balazs, A. Belyaev, and J. O'Farrill, "Direct detection of dark matter in supersymmetric models," *JCAP*, vol. 0309, p. 007, 2003.

[103] H. Baer, A. Mustafayev, S. Profumo, A. Belyaev, and X. Tata, "Direct, indirect and collider detection of neutralino dark matter in SUSY models with non-universal Higgs masses," *JHEP*, vol. 07, p. 065, 2005.

[104] J. R. Ellis, K. A. Olive, Y. Santoso, and V. C. Spanos, "On $B/s \to \mu^+\mu^-$ and cold dark matter scattering in the MSSM with non-universal Higgs masses," *JHEP*, vol. 05, p. 063, 2006.

[105] A. Corsetti and P. Nath, "Gaugino Mass Nonuniversality and Dark Matter in SUGRA, Strings and D Brane Models," *Phys. Rev.*, vol. D64, p. 125010, 2001.

[106] V. Bertin, E. Nezri, and J. Orloff, "Neutralino dark matter beyond CMSSM universality," *JHEP*, vol. 02, p. 046, 2003.

[107] R. L. Arnowitt and B. Dutta, "SUSY dark matter: Closing the parameter space," 2002.

[108] A. Birkedal-Hansen and B. D. Nelson, "Relic neutralino densities and detection rates with nonuniversal gaugino masses," *Phys. Rev.*, vol. D67, p. 095006, 2003.

[109] U. Chattopadhyay and D. P. Roy, "Higgsino dark matter in a SUGRA model with nonuniversal gaugino masses," *Phys. Rev.*, vol. D68, p. 033010, 2003.

[110] C. Pallis, "b - tau unification and sfermion mass non-universality," *Nucl. Phys.*, vol. B678, pp. 398–426, 2004.

[111] D. G. Cerdeño and C. Muñoz, "Neutralino dark matter in supergravity theories with non- universal scalar and gaugino masses," *JHEP*, vol. 10, p. 015, 2004.

[112] V. Barger *et al.*, "Recoil detection of the lightest neutralino in MSSM singlet extensions," *Phys. Rev.*, vol. D75, p. 115002, 2007.

[113] D. G. Cerdeño, C. Hugonie, D. E. Lopez-Fogliani, C. Muñoz, and A. M. Teixeira, "Theoretical predictions for the direct detection of neutralino dark matter in the NMSSM," *JHEP*, vol. 12, p. 048, 2004.

[114] D. G. Cerdeño, E. Gabrielli, D. E. Lopez-Fogliani, C. Muñoz, and A. M. Teixeira, "Phenomenological viability of neutralino dark matter in the NMSSM," *JCAP*, vol. 0706, p. 008, 2007.

[115] C. Hugonie, G. Belanger, and A. Pukhov, "Dark Matter in the Constrained NMSSM," *JCAP*, vol. 0711, p. 009, 2007.

[116] J. F. Gunion, D. Hooper, and B. McElrath, "Light neutralino dark matter in the NMSSM," *Phys. Rev.*, vol. D73, p. 015011, 2006.

[117] T. Falk, K. A. Olive, and M. Srednicki, "Heavy sneutrinos as dark matter," *Phys. Lett.*, vol. B339, pp. 248–251, 1994.

[118] N. Arkani-Hamed, L. J. Hall, H. Murayama, D. Tucker-Smith, and N. Weiner, "Small neutrino masses from supersymmetry breaking," *Phys. Rev.*, vol. D64, p. 115011, 2001.

[119] D. Hooper, J. March-Russell, and S. M. West, "Asymmetric sneutrino dark matter and the Ω_b/Ω_{DM} puzzle," *Phys. Lett.*, vol. B605, pp. 228–236, 2005.

[120] C. Arina and N. Fornengo, "Sneutrino cold dark matter, a new analysis: relic abundance and detection rates," *JHEP*, vol. 11, p. 029, 2007.

[121] C. Arina, F. Bazzocchi, N. Fornengo, J. C. Romao, and J. W. F. Valle, "Minimal supergravity sneutrino dark matter and inverse seesaw neutrino masses," *Phys. Rev. Lett.*, vol. 101, p. 161802, 2008.

[122] H.-S. Lee, K. T. Matchev, and S. Nasri, "Revival of the thermal sneutrino dark matter," *Phys. Rev.*, vol. D76, p. 041302, 2007.

[123] B. Garbrecht, C. Pallis, and A. Pilaftsis, "Anatomy of F(D)-term hybrid inflation," *JHEP*, vol. 12, p. 038, 2006.

[124] F. Deppisch and A. Pilaftsis, "Thermal Right-Handed Sneutrino Dark Matter in the F_D-Term Model of Hybrid Inflation," *JHEP*, vol. 10, p. 080, 2008.

[125] D. G. Cerdeño, C. Muñoz, and O. Seto, "Right-handed sneutrino as thermal dark matter," *Phys. Rev.*, vol. D79, p. 023510, 2009.

[126] T. Appelquist, H.-C. Cheng, and B. A. Dobrescu, "Bounds on universal extra dimensions," *Phys. Rev.*, vol. D64, p. 035002, 2001.

[127] H.-C. Cheng, K. T. Matchev, and M. Schmaltz, "Radiative corrections to Kaluza-Klein masses," *Phys. Rev.*, vol. D66, p. 036005, 2002.

[128] G. Servant and T. M. P. Tait, "Is the lightest Kaluza-Klein particle a viable dark matter candidate?," *Nucl. Phys.*, vol. B650, pp. 391–419, 2003.

[129] G. Servant and T. M. P. Tait, "Elastic scattering and direct detection of Kaluza-Klein dark matter," *New J. Phys.*, vol. 4, p. 99, 2002.

[130] H.-C. Cheng, J. L. Feng, and K. T. Matchev, "Kaluza-Klein dark matter," *Phys. Rev. Lett.*, vol. 89, p. 211301, 2002.

[131] V. K. Oikonomou, J. D. Vergados, and C. C. Moustakidis, "Direct detection of dark matter-rates for various WIMPs," *Nucl. Phys.*, vol. B773, pp. 19–42, 2007.

[132] F. Burnell and G. D. Kribs, "The abundance of Kaluza-Klein dark matter with coannihilation," *Phys. Rev.*, vol. D73, p. 015001, 2006.

[133] K. Kong and K. T. Matchev, "Precise calculation of the relic density of Kaluza-Klein dark matter in universal extra dimensions," *JHEP*, vol. 01, p. 038, 2006.

[134] S. Arrenberg, L. Baudis, K. Kong, K. T. Matchev, and J. Yoo, "Kaluza-Klein Dark Matter: Direct Detection vis-a-vis LHC," *Phys. Rev.*, vol. D78, p. 056002, 2008.

[135] B. A. Dobrescu, D. Hooper, K. Kong, and R. Mahbubani, "Spinless photon dark matter from two universal extra dimensions," *JCAP*, vol. 0710, p. 012, 2007.

[136] H.-C. Cheng and I. Low, "TeV symmetry and the little hierarchy problem," *JHEP*, vol. 09, p. 051, 2003.

[137] H.-C. Cheng and I. Low, "Little hierarchy, little Higgses, and a little symmetry," *JHEP*, vol. 08, p. 061, 2004.

[138] I. Low, "T parity and the littlest Higgs," *JHEP*, vol. 10, p. 067, 2004.

[139] A. Birkedal, A. Noble, M. Perelstein, and A. Spray, "Little Higgs dark matter," *Phys. Rev.*, vol. D74, p. 035002, 2006.

[140] J. McDonald, "Gauge Singlet Scalars as Cold Dark Matter," *Phys. Rev.*, vol. D50, pp. 3637–3649, 1994.

[141] C. P. Burgess, M. Pospelov, and T. ter Veldhuis, "The minimal model of nonbaryonic dark matter: A singlet scalar," *Nucl. Phys.*, vol. B619, pp. 709–728, 2001.

[142] M. Lisanti and J. G. Wacker, "Unification and Dark Matter in a Minimal Scalar Extension of the Standard Model," 2007.

[143] M. Cirelli, N. Fornengo, and A. Strumia, "Minimal dark matter," *Nucl. Phys.*, vol. B753, pp. 178–194, 2006.

[144] R. Barbieri, L. J. Hall, and V. S. Rychkov, "Improved naturalness with a heavy Higgs: An alternative road to LHC physics," *Phys. Rev.*, vol. D74, p. 015007, 2006.

[145] L. Lopez Honorez, E. Nezri, J. F. Oliver, and M. H. G. Tytgat, "The inert doublet model: An archetype for dark matter," *JCAP*, vol. 0702, p. 028, 2007.

[146] M. Pospelov, A. Ritz, and M. B. Voloshin, "Secluded WIMP Dark Matter," *Phys. Lett.*, vol. B662, pp. 53–61, 2008.

[147] J. R. Ellis, R. A. Flores, and J. D. Lewin, "Rates for inelastic nuclear excitation by dark matter particles," *Phys. Lett.*, vol. B212, p. 375, 1988.

[148] G. D. Starkman and D. N. Spergel, "Proposed new technique for detecting supersymmetric dark matter," *Phys. Rev. Lett.*, vol. 74, pp. 2623–2625, 1995.

[149] D. Tucker-Smith and N. Weiner, "Inelastic dark matter," *Phys. Rev.*, vol. D64, p. 043502, 2001.

[150] D. Tucker-Smith and N. Weiner, "The status of inelastic dark matter," *Phys. Rev.*, vol. D72, p. 063509, 2005.

[151] S. Chang, G. D. Kribs, D. Tucker-Smith, and N. Weiner, "Inelastic Dark Matter in Light of DAMA/LIBRA," *Phys. Rev.*, vol. D79, p. 043513, 2009.

[152] G. Belanger, E. Nezri, and A. Pukhov, "Discriminating dark matter candidates using direct detection," *Phys. Rev.*, vol. D79, p. 015008, 2009.